Continuous-Time Gray-Box Identification of Mechanical Systems Using Subspace-Based Identification Methods

Olofsson, Björn; Sörnmo, Olof; Robertsson, Anders; Johansson, Rolf

Continuous-Time Gray-Box Identification of Mechanical Systems Using Subspace-Based Identification Methods

Björn Olofsson, Olof Sörnmo, Anders Robertsson, and Rolf Johansson

Abstract— We consider the problem of gray-box identification of dynamic models for mechanical systems. In particular, the problem is approached by means of continuous-time system identification using subspace-based methods based on discrete-time input–output data. A method is developed, with the property that the structure of the model resulting from fundamental physical first principles is obtained and the parameter matrices have a clear physical interpretation. The proposed method is subsequently successfully validated in both simulation and using experimental data from a three-axis manipulator. In both cases the identified models exhibit good fit to the input–output data. The results indicate that the proposed method can be useful in the context of model-based control design in, for example, impedance force control for robots and manipulators, but also for modal analysis of mechanical systems.

I. INTRODUCTION

System identification is a fundamental part of model-based control design as well as simulation and prediction of dynamic systems. The system identification problem is to define a model structure and subsequently determine the model from input–output data acquired from experiments on the process to be investigated [1]. Typical factors to be considered concern sufficiently exciting input signals (for a measure of this property, see the notion of persistency of excitation [2]), type of model, and model order. Traditionally, three different model structures have been considered for identification; time-series models, transfer function models [3], and state-space models. Methods for identification of transfer function and time-series models include, among others, the least-squares method and the prediction-error method [2]. State-space models can be identified based on realization-based methods [4], [5] and extensions of these called subspace-based identification methods [6], [7]. Also, Bayesian Monte Carlo methods have found applications in this area recently, see [8] for algorithms for identification of nonlinear state-space models. Given the discrete-time nature of input–output data acquisition, system identification is often approached by means of discrete-time methods. However, in certain situations, in particular when considering model structures resulting from physical first principles, the dynamic relations are more natural to describe in continuous time. Considering that the transformation between a discrete-time model and a continuous-time model is not a one-to-one mapping, identification of a discrete-time model and subsequent transformation is not straightforward. Hence, algorithms for identification of continuous-time state-space models based on discrete-time experimental input–output data have been proposed, see, *e.g.*, [9], [10] for time-domain methods and [11] for frequency-domain methods.

In the modeling procedure, the models to be determined traditionally range from black-box models—*i.e.*, system models without pre-defined internal structure, where the input-output relation is the important property—to white-box models where the structure and parameters are completely determined based on first principles. A majority of the proposed system identification algorithms considers estimation of black-box models from experimental data. An intermediate model category consists of gray-box models [12], where the structure is predefined, often as a result of the physical nature of the system to be modeled, but the parameters are unknown. Here, we consider identification of gray-box models for the compliance dynamics of mechanical systems—*i.e.*, the relation between the applied force and the corresponding deflection. The motivation for the interest in this kind of models is mainly model-based control design—in particular impedance control in contact operations [13], [14] and LQ/LQG optimal state-feedback control where a physical interpretation of the states in the model is essential—but also modal analysis of mechanical systems [15]. More specifically, regarding methodology, a subspace-based identification algorithm for determining a continuous-time model from experimental data is proposed in this paper. Previous research in this area includes [16], where a black-box model approach in discrete time to the same problem was proposed. Gray-box identification for compliance dynamics and physical parameter estimation using convex optimization were investigated using frequency-based methods in [17] and identification of state-space models for compliance dynamics was treated in [18] using subspace methods in the frequency-domain. Methods for estimation of gray-box models for industrial robots have been considered in [19], and in [20] with a method based on a least-squares approach. Moreover, structural reformulations in subspace identification, similar to the one used in this paper, for general dynamic systems have been investigated in [21], [22]. The main contribution of this paper is the development and validation of a time-domain (in contrast to previously suggested frequency-domain and least-squares methods addressing the same problem) subspace-based gray-box identification method for continuous-time mechanical system models.

[1]The authors are with the Department of Automatic Control, LTH, Lund University, SE–221 00 Lund, Sweden. E–mail: bjorn.olofsson@control.lth.se.
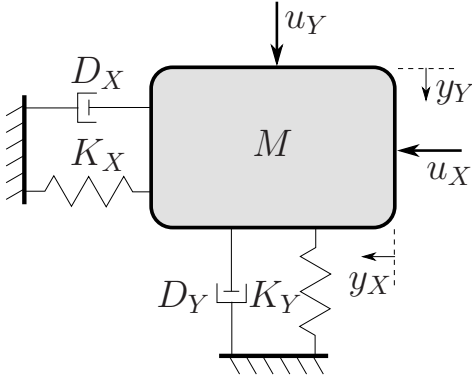
Fig. 1. Schematic depiction of a spring-mass-damper model in two dimensions, with the applied forces u_X, u_Y as inputs and the corresponding deflections y_X, y_Y as outputs.

A. Problem Formulation

Introduce the notation $M \in \mathbb{R}^{n \times n}$, $D \in \mathbb{R}^{n \times n}$, and $K \in \mathbb{R}^{n \times n}$ for the mass, damping, and stiffness matrices of the system to be modeled. From physical considerations, it is required that $M \succ 0$, $D \succeq 0$, and $K \succeq 0$, *i.e.*, the matrices are positive definite or semidefinite. The differential equations for the compliance dynamics, resulting from fundamental physical relationships, can be written as

$$M\ddot{y}(t) + D\dot{y}(t) + Ky(t) = u(t), \tag{1}$$

where $u(t) \in \mathbb{R}^n$ is the input and $y(t) \in \mathbb{R}^n$ is the output of the system, see Fig. 1. Introducing the states

$$z(t) = \begin{pmatrix} y(t) \\ \dot{y}(t) \end{pmatrix} \in \mathbb{R}^{2n}, \tag{2}$$

the following state-space system can be established

$$\dot{z}(t) = \begin{pmatrix} 0 & I \\ -M^{-1}K & -M^{-1}D \end{pmatrix} z(t) + \begin{pmatrix} 0 \\ M^{-1} \end{pmatrix} u(t), \tag{3}$$
$$y(t) = \begin{pmatrix} I & 0 \end{pmatrix} z(t).$$

Consequently, the matrices in the state-space model should have the structure indicated in (3)—*i.e.*, the following format:

$$\dot{z}(t) = \underbrace{\begin{pmatrix} 0 & I \\ A_{21} & A_{22} \end{pmatrix}}_{A} z(t) + \underbrace{\begin{pmatrix} 0 \\ B_2 \end{pmatrix}}_{B} u(t),$$
$$y(t) = \underbrace{\begin{pmatrix} I & 0 \end{pmatrix}}_{C} z(t). \tag{4}$$

The problem can then be stated as computing the matrices $\mathcal{S} : \{A \in \mathbb{R}^{2n \times 2n}, B \in \mathbb{R}^{2n \times n}, C \in \mathbb{R}^{n \times 2n}\}$ in the model based on experimentally collected sampled input–output data $\{u_k\}_{k=1}^N$ and $\{y_k\}_{k=1}^N$, where k denotes the sampling instance and uniform sampling with period h is assumed. In addition, the physical parameter matrices M, D, and K should be estimated from the identification data.

II. METHOD

In this section, the method for identification of a gray-box compliance model is described and theoretically justified.

A. Model Transformation

The system (4) is rewritten[1] using a complex variable transformation ad modum [9]. The motivation for the transformation is to avoid formulating the identification algorithm with the differential operator, which is known to be numerically challenging in the presence of noise. Applying the Laplace transform on (4) and assuming that the initial conditions are such that $z(0) = 0$, the transformed system can be written as

$$\begin{aligned} sZ(s) &= AZ(s) + BU(s), \\ Y(s) &= CZ(s). \end{aligned} \tag{5}$$

Introducing a variable transformation with the stable and causal relation

$$\lambda(s) = \frac{1}{s\tau + 1}, \quad \tau > 0, \tag{6}$$

where τ is the time constant, enables reformulation of the model to the following format

$$\begin{aligned} Z(s) &= (I + \tau A)\lambda(s)Z(s) + \tau B \lambda(s)U(s), \\ Y(s) &= CZ(s). \end{aligned} \tag{7}$$

Reformulation as an equation system in the time-domain gives

$$\begin{aligned} \xi(t) &= A_\lambda z(t) + B_\lambda u(t), \qquad z(t) = [\lambda \xi](t), \\ y(t) &= Cz(t), \end{aligned} \tag{8}$$

where $[\lambda \xi](t)$ denotes the filtered signal $\xi(t)$ and

$$A_\lambda = I + \tau A, \quad B_\lambda = \tau B, \tag{9}$$

which for the current model (4) is

$$A_\lambda = \begin{pmatrix} I & \tau I \\ \tau A_{21} & I + \tau A_{22} \end{pmatrix}, \quad B_\lambda = \begin{pmatrix} 0 \\ \tau B_2 \end{pmatrix}. \tag{10}$$

It is straightforward to derive the following relations between the output, the transformed states, and the input using recursion

$$[\lambda^{i-1}y](t) = C[\lambda^{i-1}z](t), \tag{11}$$
$$[\lambda^k y](t) = CA_\lambda^{i-1-k}[\lambda^{i-1}z](t) +$$
$$\sum_{j=k+1}^{i-1} CA_\lambda^{j-k-1}B_\lambda[\lambda^j u](t), \ 0 \le k \le i-2, \tag{12}$$

where $[\lambda^q y](t)$ means that $y(t)$ has been filtered with q serial-connected λ-filters and similarly for the input u and the state z. These relations enable the formulation of an extended linear model [9] according to

$$\mathcal{Y} = \Gamma_z \mathcal{Z} + \Gamma_u \mathcal{U}, \quad \mathcal{Z} = \left([\lambda^{i-1}z](t)\right), \tag{13}$$

with

$$\mathcal{Y} = \begin{pmatrix} [\lambda^{i-1}y](t) \\ [\lambda^{i-2}y](t) \\ \vdots \\ y(t) \end{pmatrix}, \quad \mathcal{U} = \begin{pmatrix} [\lambda^{i-1}u](t) \\ [\lambda^{i-2}u](t) \\ \vdots \\ u(t) \end{pmatrix}. \tag{14}$$

---

[1]Even though the model (1) is linear in the parameters, the derivatives of the output, $\dot{y}(t)$ and $\ddot{y}(t)$, are not available for measurement and thus a least-squares solution is not directly applicable.

Moreover, the extended observability matrix Γ_z is defined as

$$\Gamma_z = \begin{pmatrix} C \\ CA_\lambda \\ \vdots \\ CA_\lambda^{i-1} \end{pmatrix}, \tag{15}$$

and the matrix Γ_u is defined according to

$$\Gamma_u = \begin{pmatrix} 0 & 0 & \cdots & 0 \\ CB_\lambda & 0 & \cdots & \vdots \\ \vdots & \vdots & \ddots & 0 \\ CA_\lambda^{i-2}B_\lambda & CA_\lambda^{i-3}B_\lambda & \cdots & 0 \end{pmatrix}. \tag{16}$$

Remark 1: The noise component of the dynamic model has been omitted in the transformation presented here due to space limitations. For details regarding the transformation of the noise component and representation of the model on innovations form, see [9].

B. Subspace Identification

The identification of the matrices $\{A_\lambda, B_\lambda, C\}$ is based on the N4SID subspace algorithm [7], [23]. However, to accommodate the predefined structure of the system to be identified, certain modifications are made. The filtered discrete-time input–output data are collected in the matrices (similar to the Hankel matrices in the discrete-time case)

$$\mathcal{U}_N = \begin{pmatrix} [\lambda^{i-1}u]_1 & [\lambda^{i-1}u]_2 & \cdots & [\lambda^{i-1}u]_N \\ [\lambda^{i-2}u]_1 & [\lambda^{i-2}u]_2 & \cdots & [\lambda^{i-2}u]_N \\ \vdots & \vdots & \ddots & \vdots \\ [\lambda u]_1 & [\lambda u]_2 & \cdots & [\lambda u]_N \\ u_1 & u_2 & \cdots & u_N \end{pmatrix}, \tag{17}$$

where the sampled and filtered input at time t_k is denoted $[\lambda^q u]_k$ and an analogous construction $\mathcal{Y}_N$ is made for the filtered outputs $[\lambda^q y]_k$. Estimates of the system matrices $\hat{A}_\lambda$ and $\hat{C}$ are then computed using Step 1–5 of Algorithm 4.8 in [23], which provides the matrices up to a similarity transform. In order to fix the state space such that the desired form of the model in (4) is obtained, a state transformation $z \to Tz$, $T \in \mathbb{R}^{2n \times 2n}$, is made. Partition the state matrix estimates according to

$$\hat{A}_\lambda = \begin{pmatrix} \hat{A}_\lambda^{11} & \hat{A}_\lambda^{12} \\ \hat{A}_\lambda^{21} & \hat{A}_\lambda^{22} \end{pmatrix}, \quad \hat{C} = \begin{pmatrix} \hat{C}_1 & \hat{C}_2 \end{pmatrix}, \tag{18}$$

and then form the matrix T as follows

$$T = \begin{pmatrix} T_{11} & T_{12} \\ T_{21} & T_{22} \end{pmatrix}, \tag{19}$$

where

$$T_{11} = \hat{C}_1, \quad T_{12} = \hat{C}_2, \tag{20}$$

$$T_{21} = \frac{1}{\tau}(\hat{C}_1\hat{A}_\lambda^{11} + \hat{C}_2\hat{A}_\lambda^{21} - \hat{C}_1), \tag{21}$$

$$T_{22} = \frac{1}{\tau}(\hat{C}_1\hat{A}_\lambda^{12} + \hat{C}_2\hat{A}_\lambda^{22} - \hat{C}_2). \tag{22}$$

Based on the determined transformation matrix T, the estimated matrices $\hat{A}_\lambda$ and $\hat{C}$ are recomputed according to $\hat{A}_\lambda \to T\hat{A}_\lambda T^{-1}$ and $\hat{C} \to \hat{C}T^{-1}$. The transformed matrix $\hat{A}_\lambda$ then has the desired structure according to (10) and $\hat{C} = \begin{pmatrix} I & 0 \end{pmatrix}$. The extended observability matrix Γ_z and the estimates of the state sequence are subsequently recomputed based on the transformed estimates of the system matrices A_λ and C. Using the recomputed matrix Γ_z and recomputed state estimates, the matrix B_λ is determined by solving the least-squares problem in Step 6 of Algorithm 4.8 in [23], with the additional constraint that the matrix should have the structure specified in (10). The upper sub-block B_λ^1 of the matrix should be zero. Moreover, given that the matrix M is positive definite—and consequently the inverse M^{-1} as well—it is clear that the lower sub-block B_λ^2 should be positive definite, *i.e.*, $B_\lambda^2 \succ 0$. These constraints are straightforward to enforce, since the determination of the estimate of the matrix B_λ is performed by solving a least-squares problem. The convexity is preserved when adding the linear constraint that the upper block of the matrix should be zero and the constraint that the lower block should be positive definite. As the final step, estimates of the original continuous-time system matrices $\hat{A}$ and $\hat{B}$ are determined from $\hat{A}_\lambda$ and $\hat{B}_\lambda$ using the bijective relations in (9). The final matrices then have the structure according to (4).

Remark 2: The proposed method is not limited to the N4SID subspace algorithm. Other suggested algorithms, such as the MOESP algorithm [6] or CVA algorithm [24], can be modified for this gray-box identification purpose as well. The fundamental property is that the algorithm is organized such that the system matrices are estimated in two main steps; the first computing the matrices A_λ and C to allow for fixing the state space on the desired form, and then subsequently determine the matrix B_λ based on the recomputed extended observability matrix and estimated state sequence.

Remark 3: Analogously to the model transformation procedure in Sec. II-A, the noise model identification part has been omitted due to space limitations. However, identification of this part is possible based on an innovations form description of the continuous-time model, see [9] for details.

C. Physical Parameter Estimation

In order to retrieve the physical parameter matrices, the mass matrix M is first estimated from the matrix B in the identified state-space model. It follows directly that the estimate is given by $\hat{M} = \hat{B}_2^{-1}$, which is positive definite because of the constraint enforced in the system identification procedure in Sec. II-B. With the mass matrix M estimated, the stiffness matrix K and damping matrix D are computed from the corresponding estimated sub-blocks $\hat{A}_{21}$ and $\hat{A}_{22}$ in the system matrix according to

$$\begin{array}{ll} \underset{K}{\text{minimize}} & ||K + \hat{M}\hat{A}_{21}||_F \\ \text{subject to} & K \succeq 0 \end{array}, \tag{23}$$

and

$$\begin{array}{ll} \underset{D}{\text{minimize}} & ||D + \hat{M}\hat{A}_{22}||_F \\ \text{subject to} & D \succeq 0 \end{array}, \tag{24}$$
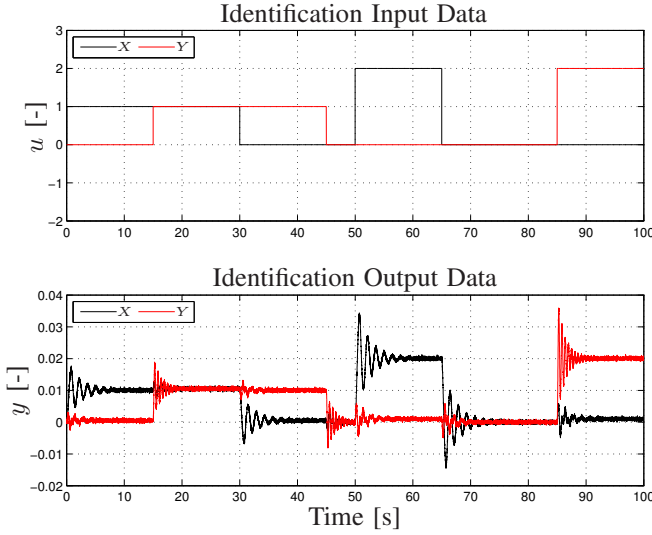
Fig. 2. Simulated input–output identification data for the system with parameters in (25).

Fig. 3. Comparison of validation output data for the system with parameters in (25) and the output from the estimated system model.

where $||\cdot||_F$ denotes the Frobenius norm. Positive semidefinite requirements are imposed on K and D when solving the corresponding optimization problems. It is straightforward to verify that the problems (23)–(24) are convex [25], and that a global minimum thus exists for each problem.

III. SIMULATION RESULTS

In order to verify the proposed approach to gray-box identification, simulated input–output data were determined from the multi-input multi-output (MIMO) system (3) with $n = 2$ and the physical parameters chosen as follows

$$
M = \begin{pmatrix} 5 & -1 \\ -1 & 1 \end{pmatrix}, \quad D = \begin{pmatrix} 5 & -0.01 \\ -0.01 & 1 \end{pmatrix},
$$
$$
K = \begin{pmatrix} 100 & -5 \\ -5 & 100 \end{pmatrix}. \tag{25}
$$

Two data sequences were simulated; one for identification and one for cross-validation. Each sequence contained a total of $N = 20000$ samples of input–output data with step inputs and a sampling period of $h = 0.005$ s, see Fig. 2 for visualization of the identification data. In addition, noise e_k was added to the measurements y from the distribution $e_k \in \mathcal{N}(0, \sigma^2 I)$ with $\sigma = 3\cdot10^{-4}$. The system can be considered as a two-dimensional spring-mass-damper system, with actuation along two directions X and Y, see Fig. 1.

A. System Identification

The system matrices A, B, and C in a state-space model of order four were estimated based on the method proposed in Sec. II, with the time constant in the variable transformation (6) chosen as $\tau = 0.15$ based on an iterative procedure. The convex optimization problems inherent in the identification procedure were solved using CVX [26], [27] in MATLAB. Moreover, the maximum order of the filtering was selected
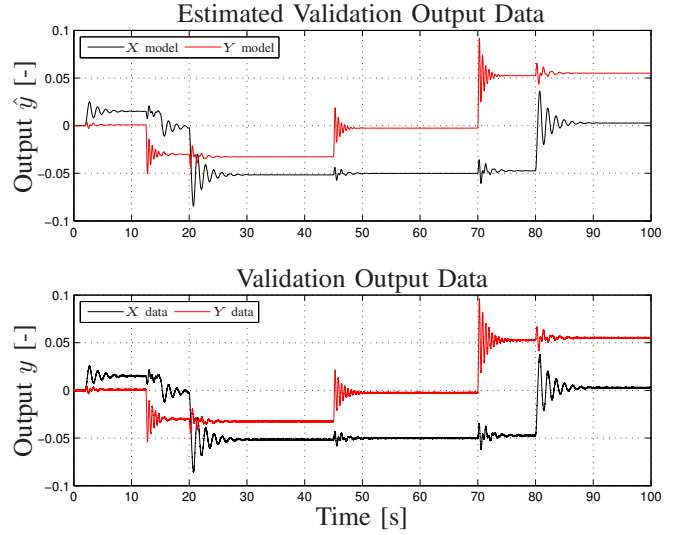
as $i = 10$. The estimated system matrices are

$$
\hat{A} = \begin{pmatrix} 0 & 0 & 1.00 & 0 \\ 0 & 0 & 0 & 1.00 \\ -24.4683 & -24.6485 & -1.3939 & -0.3884 \\ -19.1801 & -128.1179 & -1.3851 & -1.9230 \end{pmatrix},
$$
$$
\hat{B} = \begin{pmatrix} 0 & 0 \\ 0 & 0 \\ 0.2582 & 0.2590 \\ 0.2590 & 1.2926 \end{pmatrix}, \quad \hat{C} = \begin{pmatrix} 1.00 & 0 & 0 & 0 \\ 0 & 1.00 & 0 & 0 \end{pmatrix}.
$$

The validation data inputs were used as input to the estimated system with matrices $\hat{A}$, $\hat{B}$, and $\hat{C}$. A comparison of the validation data from the real system and the corresponding output $\hat{y}$ from the estimated system is shown in Fig. 3. As a measure of the fit of the estimated model to the validation data, the normalized root-mean square error (NRMSE) values (a value in the interval 0–100%, with increasing values indicating higher model fit) given by

$$
\text{NRMSE} = 100 \times \left(1 - \frac{||\mathcal{W}_N - \widehat{\mathcal{W}}_N||_2}{||\mathcal{W}_N - \overline{\mathcal{W}}_N||_2} \right) \%, \tag{26}
$$

where $\mathcal{W}_N$ is the validation output data, $\widehat{\mathcal{W}}_N$ is the output from the estimated system and $\overline{\mathcal{W}}_N$ is the mean of the validation output data, were computed for the respective axis X and Y. The values are 97.6% and 96.9%, respectively, which must be considered as good fit of the model to the validation data. To further compare the frequency characteristics of the real and the estimated models, the Bode diagrams are shown in Fig. 4. Also here it is clear that the estimated system captures the essential dynamics of the original system, where in particular the natural eigenfrequencies and the zeros of the system are identified with high accuracy.

B. Physical Parameters

To the purpose of estimating the physical parameters of the system, the mass matrix M was determined using the
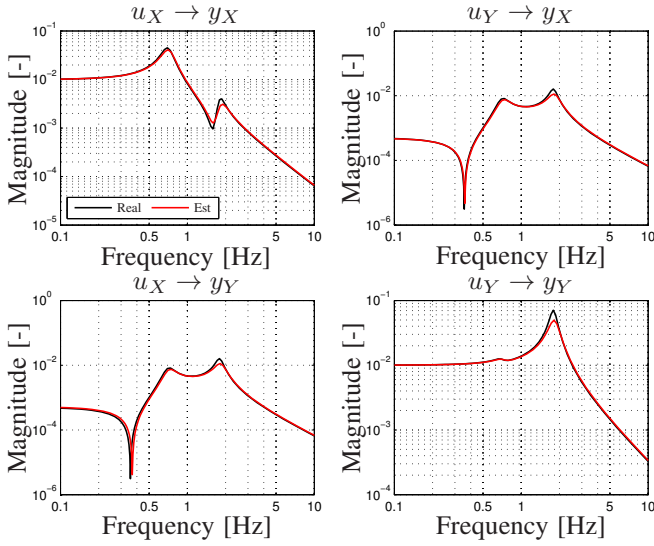
Fig. 4. Comparison of Bode diagrams of the real system with parameters in (25) and the estimated MIMO model.

procedure proposed in Sec. II-C. Based on $\hat{M}$, the estimates $\hat{K}$ and $\hat{D}$ of the stiffness matrix and the damping matrix, respectively, were computed by solving the optimization problems (23) and (24). For evaluation of the estimation accuracy, the obtained matrices are compared to the corresponding parameters for the real system in (25). The relative differences, measured with the Frobenius norm, are given by

$$\frac{||M - \hat{M}||_F}{||M||_F} = 0.0303, \quad \frac{||D - \hat{D}||_F}{||D||_F} = 0.125,$$

$$\frac{||K - \hat{K}||_F}{||K||_F} = 0.00108.$$

This indicates that also the mass matrix M and stiffness matrix K have been estimated with high accuracy and the damping matrix D with good accuracy.

IV. EXPERIMENTAL RESULTS

The proposed identification method was further evaluated on data from an experimental setup. The considered system is a piezo-actuated 3D compensation mechanism (micro manipulator) for robotic machining scenarios [28], with actuation along a Cartesian coordinate system, see Fig. 5. The mechanical design comprises solid-state joints including flexure elements, which makes the system exhibiting significant resonances at particular eigenfrequencies. Moreover, two of the axes, X and Z exhibit a noticeable coupling because of the mechanical design of the mechanism. This coupling was investigated using the approach to gray-box identification proposed in Sec. II. Consequently, a MIMO system with the actuation forces u as inputs and the corresponding displacements y_X and y_Z along the X and Z axes, respectively, was identified. Since the actuating forces were not available for explicit measurement, it was assumed that the extensions of the piezo-actuators are proportional to the forces. Two sequences of experimental data were collected with a sampling period of $h = 0.0001$ s; one of the sets was
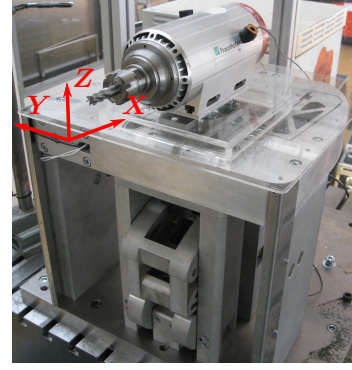

Fig. 5. Micro manipulator (developed at Fraunhofer IPA, Germany [28]) used for evaluation of the proposed identification method.
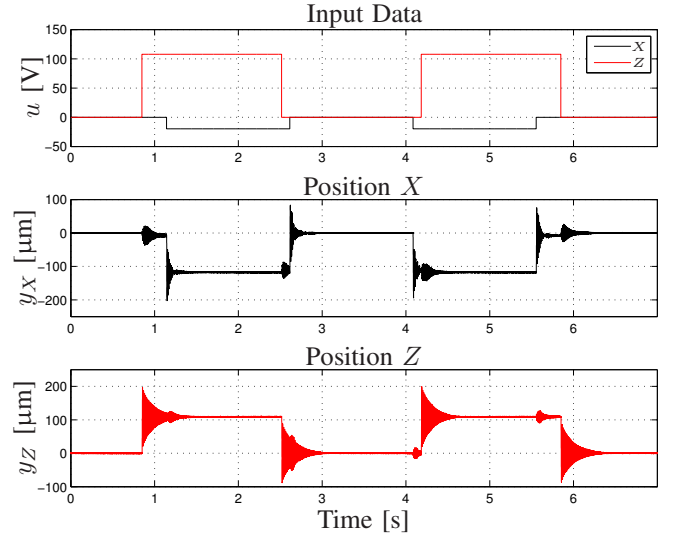

Fig. 6. Experimental input–output data for the micro manipulator. The dynamic coupling between the X- and Z-axes is clearly visible.

used as identification data and the other set was used for cross-validation purposes. The sample rate was motivated by the observed natural eigenfrequencies, obtained by spectral analysis, in the order of 100 Hz and the fact that the data were to be processed with low-pass filters in the identification procedure. The inputs to the mechanical system were a sequence of steps with randomly chosen time distance. The Cartesian extension of the end-effector was measured using capacitive sensors and the collected experimental input–output data were detrended prior to system identification. The resulting identification data are displayed in Fig. 6.

A. System Identification

A MIMO model of the micro manipulator of fourth order was estimated with the method in Sec. II, using the identification data shown in Fig. 6. The time constant $\tau = 0.00314$ was used in the operator transformation (6) for accommodating the frequency properties of the system at hand. The time constant was found by employing a linear search over a predefined interval and evaluating the corresponding model fit for the identification data series for each of the filter time constants. Moreover, the maximum
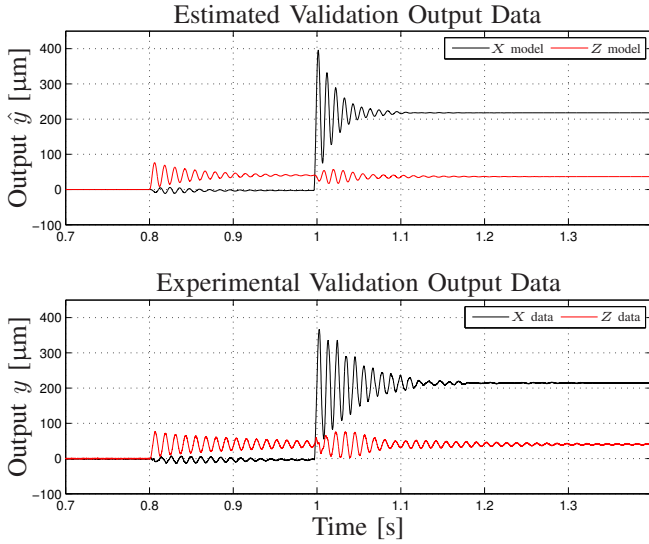
Fig. 7. Comparison of experimental validation output data for the micro manipulator and the output from the estimated system model.

Fig. 8. Bode diagram of the estimated MIMO-model for the micro manipulator.

filter order was selected as $i = 8$. For cross-validation of the estimated micro manipulator model, the validation data series (containing a sequence of step inputs different from the identification data series) was used. The experimental validation output data and the corresponding output $\hat{y}$ from the estimated model for the same input signals are displayed in Fig. 7 for a segment of the data series used. The NRMSE values for the computed model are 88.8% and 73.6% for the X and Z-axis, respectively, which indicates that the essential dynamics of the system are captured. The dynamics not captured by the model can be explained by higher-order harmonics, arising because of the nonlinear dynamics of the piezo-actuators used in the micro manipulator design.

The frequency characteristics of the estimated model are represented in the Bode diagram in Fig. 8. The natural eigen-frequencies observed at 96.6 Hz and 83.0 Hz for the X- and Z-axis, respectively, correspond well to the eigenfrequencies extracted using spectral analysis of the experimental data. It is interesting to observe that it is the resonance along the Z-axis that results in the cross coupling between the axes—*i.e.*, actuation along the Z-axis results in oscillations along the X-axis as well with the eigenfrequency of the former.

B. Physical Parameters

The mass matrix M was estimated from the matrix $\hat{B}$ in the state-space model for the micro manipulator. Moreover, using the system matrix $\hat{A}$ in the model and the mass-matrix estimate $\hat{M}$, the stiffness matrix K and the damping matrix D were estimated as described in Sec. II-C. The estimates of the physical parameters are given by

$$\hat{M} = 1.0 \cdot 10^{-5} \begin{pmatrix} 0.0487 & 0.0001 \\ 0.0001 & 0.3669 \end{pmatrix},$$

$$\hat{D} = 1.0 \cdot 10^{-3} \begin{pmatrix} 0.0407 & 0.0302 \\ 0.0302 & 0.1484 \end{pmatrix}, \quad (27)$$

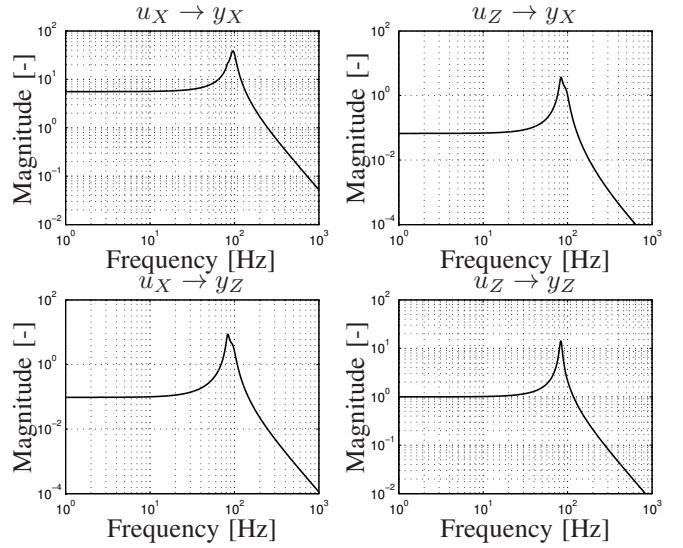$$\hat{K} = \begin{pmatrix} 0.1793 & 0.0147 \\ 0.0147 & 1.0049 \end{pmatrix}. \quad (28)$$

In the modal analysis procedure, the generalized eigenval-ues ω resulting in non-trivial solutions v (*i.e.*, generalized eigenvectors) to the equation $Kv = \omega^2 Mv$ are of interest since they correspond to the eigenmodes of the system. In particular, the eigenfrequencies are given by ω. Solving the generalized eigenvalue problem for the estimated mass and stiffness matrices gave the eigenfrequencies $\omega_1 = 96.7$ Hz and $\omega_2 = 83.1$ Hz, which is well in agreement with the eigenfrequencies observed in the Bode diagram in Fig. 8.

V. DISCUSSION

We have considered gray-box identification of linear mod-els for mechanical systems. The characterization of the dynamic force–deflection relationships does not only provide information about the mechanical system as such, but is also essential for model-based control design. Important examples here are contact operations for robot manipulators in man-ufacturing scenarios such as machining, which successfully have been executed using impedance force control [13].

Using subspace-based methods for identification in this context is natural, since the systems to be modeled are of MIMO character, and in addition subspace methods have been found to be advantageous when modeling systems with closely spaced natural eigenfrequencies (and thus resulting resonances) [29]. Since this is often the case with mechanical systems—*cf.* the micro manipulator system investigated in Sec. IV—this is an essential property of the method.

In order to allow for continuous-time identification in the time-domain (in contrast to previous suggested methods in the frequency-domain), a variable transformation was made in (6). This transformation includes the choice of the filter time constant τ. During the development of the method proposed in this research, the choice of this constant has been found essential in order to obtain models with satisfactory fit to the data and even stability. Intuitively, it is natural that the frequency content of the experimental identification data and the sampling rate of the same have implications on the

choice. In the experimental results presented in Sec. IV, a linear search was used for finding the time constant maximizing the fit to the identification data in a pre-defined interval. Another option is to use multiple time constants in a logarithmically spaced interval for initial examination of the identification data. A drawback with this option is that the computational complexity increases.

Another question is if it is sufficient to use linear models, since it is known that, *e.g.*, robot manipulators exhibit nonlinear stiffness when applying strong external process forces at the end-effector. In addition, configuration-dependent compliance properties are expected. First, it is plausible that linear models are appropriate as initial approximations when designing position controllers. Second, within a certain limited range of input signals in a limited Cartesian workspace, the linear approximation is indeed valid. For modeling of configuration-dependent robot compliance dynamics, linear parameter-varying models can also be considered. Moreover, a method for identification of the nonlinear static stiffness-relationship using an inexpensive measurement setup has been proposed [30].

In the problem formulation in this paper, it was assumed that all position states were available for measurements. This is a limitation when considering identification of systems with non-actuated modes whose corresponding outputs are not easily measurable. It is an interesting aspect of future research to investigate how the method can be adopted to accommodate unmeasurable position states when determining the dynamic model from the input–output data.

VI. CONCLUSIONS

This paper has proposed a method for identification of continuous-time gray-box models in the time-domain by using experimental input–output data. The method relies on subspace-based identification for computing the matrices of a state-space model and estimating the physical parameters. Moreover, the method was successfully evaluated both in simulation and in experiments, where the obtained models exhibited good fit to the data and the model-parameter matrices were feasible from a physical point-of-view.

REFERENCES

[1] R. Johansson, *System Modeling and Identification*. Englewood Cliffs, NJ: Prentice Hall, 1993.

[2] K. J. Åström and T. Bohlin, "Numerical identification of linear dynamic systems from normal operating records," in *Theory of Self-Adaptive Control Systems*. Plenum Press, 1966, pp. 96–111.

[3] H. Madsen, *Time Series Analysis*. Boca Raton, FL: Chapman & Hall/CRC, 2008.

[4] B. L. Ho and R. E. Kalman, "Effective construction of linear state-variable models from input/output functions," *Regelungstechnik*, vol. 14, no. 12, pp. 545–592, 1966.

[5] J.-N. Juang and R. S. Pappa, "An eigensystem realization algorithm for modal parameter identification and model reduction," *J. Guidance, Control, and Dynamics*, vol. 8, no. 5, pp. 620–627, 1985.

[6] M. Verhaegen and P. Dewilde, "Subspace model identification—The output-error state-space model identification class of algorithms," *Int. J. Control*, vol. 56, pp. 1187–1210, 1992.

[7] P. van Overschee and B. De Moor, "N4SID: Subspace algorithms for the identification of combined deterministic-stochastic systems," *Automatica*, vol. 30, no. 1, pp. 75–93, 1994.

[8] T. Schön, A. Wills, and B. Ninness, "System Identification of Nonlinear State-Space Models," *Automatica*, vol. 47, no. 1, pp. 39–49, 2011.

[9] R. Johansson, M. Verhaegen, and C. T. Chou, "Stochastic theory of continuous-time state-space identification," *IEEE Trans. Signal Process.*, vol. 47, pp. 41–51, 1999.

[10] B. R. J. Haverkamp, M. Verhaegen, C. T. Chou, and R. Johansson, "Continuous-time identification of MIMO state-space models from sampled data," in *Proc. IFAC Symp. System Identification (SYSID)*, Kitakyushu, Fukuoka, Japan, 1997.

[11] T. McKelvey, H. Akay, and L. Ljung, "Subspace-based multivariable system identification from frequency response data," *IEEE Trans. Autom. Control*, vol. 41, no. 7, pp. 960–979, 1996.

[12] T. Bohlin, "A case study of grey box identification," *Automatica*, vol. 30, no. 2, pp. 307–318, 1994.

[13] N. Hogan, "Impedance control: An approach to manipulation: Parts I-III," *ASME J. Dynamic Systems, Measurement, and Control*, vol. 107, pp. 1–24, 1985.

[14] T. Olsson, R. Johansson, and A. Robertsson, "Flexible force-vision control for surface following using multiple cameras," in *Proc. IEEE/RSJ Int. Conf. Intelligent Robots and Systems (IROS)*, Sendai, Japan, 2004, pp. 798–803.

[15] W. Heylen, S. Lammens, and P. Sas, *Modal Analysis Theory and Testing*. Heverlee, Belgium: Katholieke Universiteit Leuven, 1997.

[16] M. Cescon, I. Dressler, R. Johansson, and A. Robertsson, "Subspace-based identification of compliance dynamics of parallel kinematic manipulator," in *Proc. IEEE/ASME Int. Conf. Advanced Intelligent Mechatronics*, Singapore, 2009, pp. 1028–1033.

[17] X. Tan, H. Tanaka, and Y. Ohta, "Grey-box modeling of rotary type pendulum system with position-variable load," in *Proc. IFAC Symp. System Identification (SYSID)*, Brussels, Belgium, 2012, pp. 1263–1268.

[18] A. Cavallo, G. De Maria, C. Natale, and S. Pirozzi, "Gray-box identification of continuous-time models of flexible structures," *IEEE Trans. Control Syst. Technol.*, vol. 15, no. 5, pp. 967–981, 2007.

[19] E. Wernholt and S. Moberg, "Nonlinear Gray-Box Identification Using Local Models Applied to Industrial Robots," *Automatica*, vol. 47, no. 4, pp. 650–660, 2011.

[20] M. Gautier, "Numerical calculation of the base inertial parameters of robots," *J. Robotic Systems*, vol. 8, no. 4, pp. 485–506, 1991.

[21] C. Lyzell, "Structural Reformulations in System Identification," Linköping Studies in Science and Technology. Dissertations No. 1475, Linköping University, Sweden, 2012.

[22] C. Lyzell, M. Enqvist, and L. Ljung, "Handling certain structure information in subspace identification," in *Proc. IFAC Symp. System Identification (SYSID)*, Saint-Malo, France, 2009, pp. 90–95.

[23] P. Van Overschee and B. De Moor, *Subspace Identification for Linear Systems—Theory, Implementation, Applications*. Boston, London, Dordrecht: Kluwer Academic Publishers, 1996.

[24] W. E. Larimore, "Canonical variate analysis in identification, filtering, and adaptive control," in *Proc. IEEE Conf. Decision and Control (CDC)*, Honolulu, HI, 1990, pp. 596–604.

[25] S. P. Boyd and L. Vandenberghe, *Convex Optimization*. Cambridge, England: Cambridge University Press, 2004.

[26] CVX Research Inc., "CVX: Matlab software for disciplined convex programming, version 2.0 beta," http://cvxr.com/cvx, 2014.

[27] M. Grant and S. Boyd, "Graph implementations for nonsmooth convex programs," in *Recent Advances in Learning and Control*, V. Blondel, S. Boyd, and H. Kimura, Eds. Springer-Verlag, Berlin Heidelberg, 2008, pp. 95–110.

[28] O. Sörnmo, B. Olofsson, U. Schneider, A. Robertsson, and R. Johansson, "Increasing the milling accuracy for industrial robots using a piezo-actuated high-dynamic micro manipulator," in *Proc. IEEE/ASME Int. Conf. Advanced Intelligent Mechatronics (AIM)*, Kaohsiung, Taiwan, 2012, pp. 104–110.

[29] R. Johansson, A. Robertsson, K. Nilsson, and M. Verhaegen, "State-space system identification of robot manipulator dynamics," *Mechatronics*, vol. 10, no. 3, pp. 403–418, 2000.

[30] C. Lehmann, B. Olofsson, K. Nilsson, M. Halbauer, M. Haage, A. Robertsson, O. Sörnmo, and U. Berger, "Robot joint modeling and parameter identification using the clamping method," in *Proc. IFAC Conf. Manufacturing Modelling, Management, and Control (MIM)*, St. Petersburg, Russia, 2013, pp. 843–848.